Spectroscopy of ^{52}Mn via the ^{54}Fe$(d,\alpha)^{52}$Mn Reaction and the ^{52}Cr$(p, n\gamma)^{52}$Mn Coincidence Experiment*

R. M. DelVecchio†
Nuclear Physics Laboratory, University of Pittsburgh, Pittsburgh, Pennsylvania 15213
(Received 2 October 1972)

The ^{54}Fe$(d,\alpha)^{52}$Mn reaction was studied at 17-MeV bombarding energy. Energy assignments based on the (d,α) and two $(^3\text{He},t)$ spectra were made for some 60 levels up to about 4 MeV of excitation in ^{52}Mn with accuracies ranging from ±1 to ±10 keV. (d,α) L-transfer assignments or suggestions were made for 28 of these levels based on a recent distorted-wave Born-approximation procedure. Spin-parity limits based on the (d,α) analysis are generally in agreement with other work although a few discrepancies are noted. The ^{52}Cr$(p,n\gamma)$-^{52}Mn coincidence experiment was performed at bombarding energies of 8.0, 8.5, 9.0, 9.5, and 10.0 MeV. 30 γ rays were fitted into a decay scheme which includes four previously unreported levels below 1.3 MeV of excitation in ^{52}Mn. Two of these new levels were weakly excited in (d,α), while the other two appeared as an unresolved group in the $(^3\text{He},t)$ spectra. Since the γ-rays were observed with 3-keV Ge(Li) detector resolution, accurate energy assignments ($\leq$±0.5 keV) could be made for 14 levels in ^{52}Mn. The γ-ray data are consistent with the (d,α) spin limits. A comparison of the low-lying states with the McCullen, Bayman, and Zamick calculations is presented. The four new levels do not fit into the pure $f_{7/2}$-shell scheme.

INTRODUCTION

The $f_{7/2}$ shell is an especially interesting shell because of the abundance of experimentally accessible nuclei which in first-order shell-model theory have both their valence protons and neutrons in this shell. The pure $f_{7/2}$-shell model calculations of McCullen, Bayman, and Zamick (MBZ)[1] have enjoyed a high degree of success. The relative isolation of the $f_{7/2}$ shell from neighboring shells suggests that the mixing of other configurations would not drastically alter the pure $f_{7/2}$-model results at low excitation. One therefore expects reasonable but not perfect agreement of the experimental data with the MBZ predictions. Because of the relatively high density of low-lying states which odd-odd $f_{7/2}$-shell nuclei enjoy, they afford a valuable testing ground for MBZ or future theoretical ideas. ^{52}Mn, having five protons and seven neutrons in the $f_{7/2}$ shell, presents itself as both a theoretical and experimental challenge. Its expected high-level density requires that it be studied with good energy resolution, while target availability requires that it be studied with at least a two-nucleon transfer or charge-exchange reaction. The (d,α) reaction was chosen because of the selection rule which forbids the pickup of a deuteron of the $(l_j)^2$ configuration coupled to an even spin, assuming a direct reaction mechanism.[2] Hence the low-lying even-spin states in ^{52}Mn would be excited only to the extent of configuration mixing and should be weak compared with odd-spin states of the $f_{7/2}$ configuration. The $(p,n\gamma)$ reaction was performed in order to determine excitation energies more accurately, to look for states possibly missed in (d,α), and to provide a consistency check on the (d,α) spin limits or assignments.

Previous (d,α) experiments[3,4] have not been done with as good a resolution as was possible in this work (15 keV) and have consequently missed many of the levels reported here. By the use of a new distorted-wave Born-approximation (DWBA) procedure,[5] it was hoped that L-transfer assignments could be made with little ambiguity. The ^{52}Cr$(p,n\gamma)^{52}$Mn experiment has not been previously reported.

^{54}Fe$(d,\alpha)^{52}$Mn EXPERIMENT

A. Experimental Procedure

The (d,α) experiment was performed with a 17-MeV deuteron beam from the University of Pittsburgh Van de Graaff accelerator. Targets were made by evaporation of the ^{54}Fe metal onto thin (20-μg/cm^2) carbon backings to thicknesses of ~50 μg/cm^2. The isotopic purity of the ^{54}Fe was only 92% so that interfering peaks, mainly from the ^{56}Fe$(d,\alpha)^{54}$Mn reaction, appeared in the spectra. Most of these impurity peaks were identified by the use of a natural Fe target, however the background created by the relatively high density of these states made it difficult to analyze any but the stronger ^{52}Mn states especially at high

excitation. α particles were detected on Ilford K-1 plates placed in the focal plane of the Enge split-pole spectrograph, except for the small-angle ($\leq 20°$) runs where position-sensitive detectors were employed. Absolute cross sections were determined by (a) the use of Rutherford scattering to measure the target thickness directly and (b) the use of NaI monitors in the spectrograph scattering chamber to detect the elastic deuterons. Both methods agreed to better than 15% which is the estimated absolute cross-section error. Relative cross sections were based mainly on charge monitoring. The energy resolution achieved was 15 keV full width at half maximum (FWHM) over all.

B. Energy Determinations

Excitation energies were determined by using a known spectrum to calibrate the focal plane at the angle and focal plane settings used for ^{52}Mn. The ^{58}Ni$(d, \alpha)^{56}$Co reaction was chosen to obtain a calibration spectrum, since many ^{56}Co level energies were known to high precision.[6,7] This method was applied at two angles for the (d, α) reaction. It was also applied to the ^{52}Cr$(^3$He, $t)^{52}$Mn reaction at two angles; however, in this case the levels of ^{53}Mn[8,9] which appeared simultaneously on the plates via the ^{52}Cr$(^3$He, $d)^{53}$Mn reaction were used to calibrate the focal plane. Triton peaks could be identified by using enough absorber to stop them but not the deuterons and noting which peaks were absent in the resulting spectrum. The computer code SPIRO[10] did the necessary calculations, including target thickness corrections. The first column in Table I shows the averaged energies and their errors obtained by the above techniques. These energies agree within the errors for levels previously studied, especially with the more accurate determinations of Refs. 11 and 12. A portion of a (d, α) plate spectrum is shown in Fig. 1. Peaks of ^{52}Mn are labeled by their energy, while unlabeled peaks are from target impurities. $(^3$He, $t)$ cross sections at $40°_{\text{lab}}$ are shown in Table I. These were based on the $E_{^3\text{He}} = 19$ MeV plate spectrum and a position-sensitive detector run at 18 MeV. The latter technique was used to gate out the deuteron peaks which seriously obscured the triton peaks at higher excitation. The variation of the cross sections with energy is known to be small in this energy region.[13] The cross-section errors are estimated to be ±25%.

C. Excitation Functions

A previous (d, α) study[4] at $E_d = 15$ MeV indicated the possible presence of compound reaction effects in the angular distributions. Using a self-supporting ^{54}Fe foil of ~0.5-mg/cm^2 thickness and employing solid-state detectors and monitors, (d, α) excitation functions were taken in our 24-in. scattering chamber. Detectors were placed at several angles and the beam was varied in 200-keV steps from 14.2 to 16.8 MeV. Since the resolution achieved was 60 keV and background became a problem at higher excitation, only the levels shown in Fig. 2 were analyzed. For these levels, fluctuations are not apparent so that compound effects are probably small. Because the target was ~20 keV thick, fluctuations of less than this energy spacing cannot be ruled out.

D. DWBA Procedure

A DWBA procedure which has been successful in fitting a wide range of (d, α) reactions[5] was employed. This technique requires that the real geometries of both the deuteron and α optical potentials be the same. In particular, the restrictions

$$r_0 = 1.2 \text{ fm},$$
$$a_0 = 0.75 \text{ fm},$$
$$V_0 \cong n V_{\text{nucleon}},$$

were used, where n is the number of nucleons in the projectile and V_{nucleon} is the single-nucleon potential ($\cong 50$ MeV). These restrictions remove some of the optical-parameter ambiguities while still permitting good fits to the elastic data. Optical parameters based on this procedure are shown in Table II. Although these parameters are applicable to neighboring nuclei, the use of ^{52}Cr elastic deuteron parameters gave similar (d, α) predictions. The code DWUCK[14] was used to generate the (d, α) angular distributions. Various DWUCK options were tried: (a) the cluster deuteron description using the parameters $r_0 = 1.2$ fm and $a_0 = 0.75$ fm for the bound deuteron well. This description was used with and without finite-range corrections. (b) The microscopic description with the bound well parameters $r_0 = 1.25$ fm and $a_0 = 0.75$ fm for the single-particle wells. This description was tried only with finite range. The finite-range parameter used was $R = 0.4$[15] and the standard nonlocality parameters ($\beta_d = 0.54$, $\beta_\alpha = 0.2$) were employed. Figure 3 shows the results for several L transfers. As expected from Ref. 5 the finite-range correction has a small effect on the angular distribution shapes. In view of the close similarity of all curves, the curves generated by procedure (b) were used to fit the experimental data. Since

TABLE I. ^{52}Mn spectroscopic data.

	This work ^{54}Fe$(d, \alpha)^{52}$Mn 17 MeV			19 MeV (^{3}He, t)	Ref. 3	Ref. 4	Ref. 12	Ref. 13		
Exc. (keV)	σ(30°) (μb/sr)	L	J^π	σ(40°) (μb/sr)	(d, α) L	(d, α) L	(^{3}He, p) L	(^{3}He, t) J^π	Ref. 18 J^π	Best J^π
0	3.0	(6)	(6$^+$)	7.2		(6)		6$^+$	6$^+$	6$^+$
378 ± 1	1.6	(2)	(2$^+$)	9.3		(2)		2$^+$	2$^+$	2$^+$
546 ± 1	10	(2)	(1$^+$, 3$^+$)	8.8		0 + 2		1$^+$	1$^+$	1$^+$
732 ± 1	2.3	4	4$^+$	6.3		(4)		4$^+$		4$^+$
826 ± 1	27	2	3$^+$	32	6	2 + 4		7$^+$		3$^+$
870 ± 1	250	6	7$^+$	36		6				7$^+$
884 ± 2	a			18						
1252 ± 1 [b]	82	4 + 6	5$^+$	12	4	4 + 6		5$^+$		5$^+$
1646 ± 2	~1.3	c								
1683 ± 1	8.5	4	3$^+$-5$^+$	2.6	4	2 + 4				3$^+$-5$^+$
1954 ± 2	3.4	6	5$^+$-7$^+$	5.0						5$^+$-7$^+$
2046 ± 4	~2.5	c		5.0						
2130 ± 5	11	4	3$^+$-5$^+$	1.5	(2)					3$^+$-5$^+$
2252 ± 2	9.8	4	3$^+$-5$^+$	3.8	4					3$^+$-5$^+$
2285 ± 5	~2.5	c								
2338 ± 2	5.0	3, 2		2.7			(2)			(1$^+$-3$^+$)
2475 ± 2	22	(0+2, 1)	(1$^\pm$, 2$^-$)		0	1 + 3	0		0$^+$, 1$^+$	(1$^+$) [d]
2.55 [e]										
2629 ± 3	40	0 + 2	1$^+$	20	0	0 + 2	0 + 2	2$^+$	0$^+$, 1$^+$	1$^+$
(2645 ± 5)				~8.0						
2667 ± 10				~2.0						
2711 ± 3	56	f		6.0	(3)	(5)				(2$^-$-6$^-$)
2785 ± 4				3.8			2			
2796 ± 3	21	(2)	(1$^+$-3$^+$)	8.3		(2)			1$^+$-3$^+$	1$^+$-3$^+$
2815 ± 4				9.4						
2848 ± 3	97	f		11	3	2 + 4		(1$^+$, 2$^+$)		
2858 ± 5				14						
2872 ± 4				4.9						
2903 ± 5	21	f		5.1		(2)	0			1$^+$
2925 ± 5				67			0	0$^+$	0$^+$	0$^+$
2955 ± 5	2.5	c		2.4						
2973 ± 4	4.4	c		4.0						
2982 ± 3										
3077 ± 4				3.2						
3106 ± 4	5.0	(2)	(1$^+$-3$^+$)	2.8						(1$^+$-3$^+$)
3199 ± 3	11.0	4	3$^+$-5$^+$	1.1		0				3$^+$-5$^+$ [d]
3226 ± 4	12	4 + (6)	(5$^+$)	1.5	2					(5$^+$) [d]
3245 [g]						(0 + 2) [e]				(1$^+$)
3297 ± 5	~3.0			2.0		(2)				(1$^+$-3$^+$)
3333 ± 3	26	(2 + 4)	(3$^+$)	5.0						(3$^+$)
3351 ± 5				3.7						
3386 ± 3	11	(2 + 4)	(3$^+$)	2.8						(3$^+$)
3423 ± 3	110	f		12	3	2				d
2490 ± 10				3.8						
3506 ± 3	46	(4)	(3$^+$-5$^+$)	4.3						(3$^+$-5$^+$)
3573 ± 5 [h]	17	0	1$^+$	4.2	(3)	0				1$^+$
3620 ± 6	3.9	c								
3640 ± 6	15	c		13						
3655 ± 6	15	f								
3706 ± 6	5.6	c								

TABLE I *(Continued)*

Exc. (keV)	This work ^{54}Fe(d, α)^{52}Mn 17 MeV σ(30°) (μb/sr)	L	J^π	19 MeV (^{3}He, t) σ(40°) (μb/sr)	Ref. 3 (d, α) L	Ref. 4 (d, α) L	Ref. 12 (^{3}He, p) L	Ref. 13 (^{3}He, t) J^π	Ref. 18 J^π	Best J^π
3738 ± 4	16	4	3^+–5^+	5.4	4					3^+–5^+
3776 [g]						2				(1^+–3^+)
3884 ± 6				3.3		(4)				(3^+–5^+)
3898 ± 4	12	(2)	(1^+–3^+)							(1^+–3^+)
3936 ± 4	3.7	c								
3973 ± 6 / 3987 ± 6	10	(4)			1, 2					
4061 ± 4	4.8	c								
4129 ± 8	2.6	4	3^+–5^+							3^+–5^+
4235 ± 8	19	c								
4281 ± 8	18	(2)	(1^+–3^+)			2				1^+–3^+
4314 [g, h]					(0, 1, 2)					
4377 ± 8	20	0 + 2	1^+			0 + 2				1^+

[a] Blanks denote levels not seen. They could possibly be weak or masked by an impurity.
[b] Seen as a doublet by Ref. 11.
[c] Insufficient statistics for L determination.
[d] Discrepancies exist.
[e] Reference 11.
[f] Structureless or unfittable angular distribution.
[g] Reference 12.
[h] Seen as a doublet by Ref. 12.

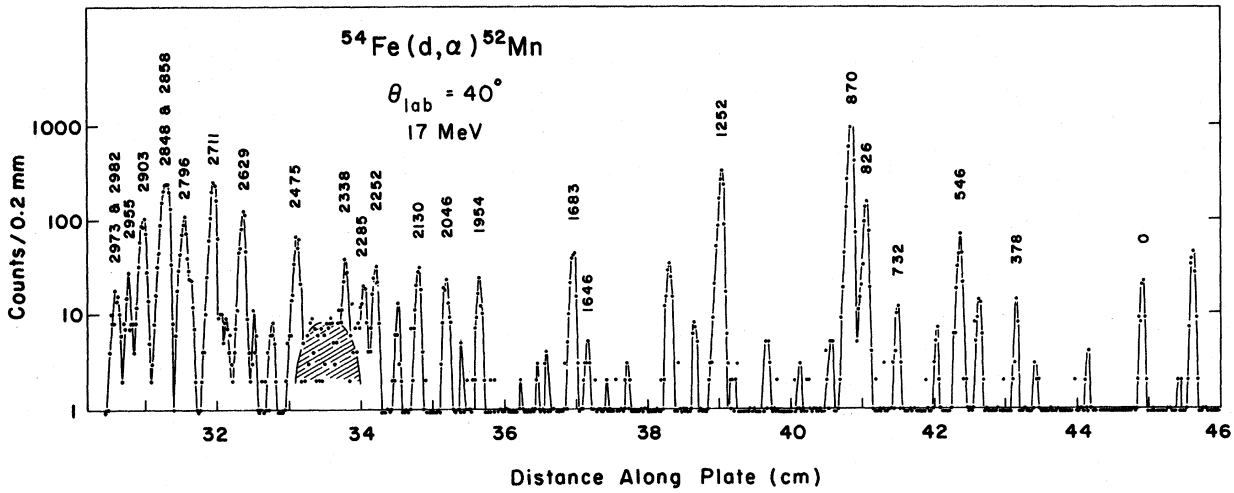

FIG. 1. Portion of an ^{54}Fe(d, α)^{52}Mn plate spectrum.

an excitation range of 4 MeV was studied, Q-value effects as shown in Fig. 4 were important. The ground-states Q value is 5.168 MeV. The experimental (d, α) angular distributions are shown in Fig. 5 (a)–(f) along with the DWBA curves calculated to the nearest 0.5 MeV of the level studied. The error bars reflect statistical and background subtraction errors.

E. Spin Limits and Assignments

The (d, α) L-transfer values are given in Table I along with the implied spin limits or assignments. When two L values contribute to the angular distribution, the spin is uniquely determined. The (d, α) cross sections at 30° c.m. shown in Table I indicate which of the low-lying states have even or odd spin, according to the $(l_j)^2$ rule mentioned previously. For the even-spin positive-parity states, $J = L$ while for odd-spin positive-parity states $J = L \pm 1$, however, the + sign is preferred by geometric-coupling considerations except for the 1^+ state. The 546-keV known 1^+ state is seen to proceed mainly by $L = (2)$ so that the coupling $J = L - 1$ seems to be preferred. Incoherent addition of $L = 0$ strength did not improve the DWBA fit to this level. Our results agree substantially with the previous work summarized in Table I, where comparisons are possible. A few discrepancies, however, are noted in the table. Divergent assignments occur at energies of 2.5 MeV and higher and may often reflect the excitation of close-lying but different states by different reactions.

^{52}Cr$(p, n\gamma)^{52}$Mn COINCIDENCE EXPERIMENT

A. Experimental Procedure

Since the signal from the neutron detector, a 5-in. diam × 3-in. cylindrical NE 213 liquid scintillator, could not be used to measure neutron energies very well except in a time-of-flight arrangement, the $(p, n\gamma)$ experiment was run at beam energies of 8.0, 8.5, 9.0, 9.5, and 10.0 MeV in order to obtain the approximate excitation region of the

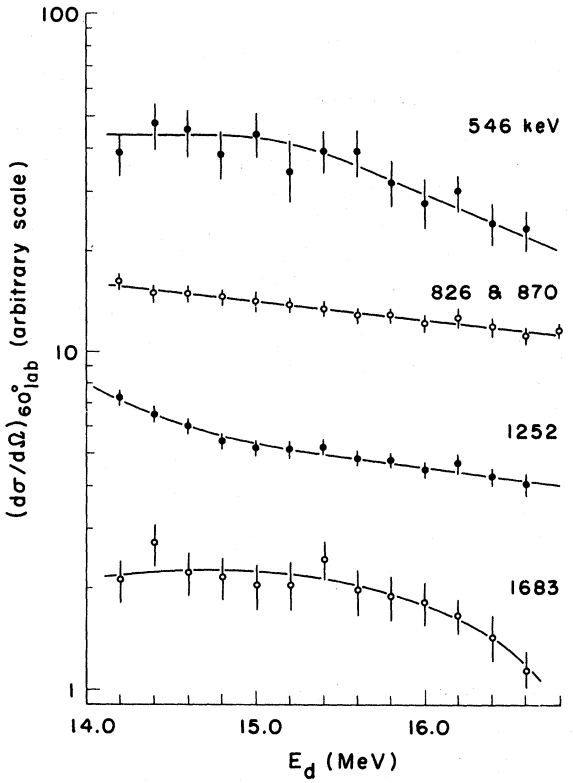

FIG. 2. ^{54}Fe$(d, \alpha)^{52}$Mn excitation functions at $\theta_{lab} = 60°$. The solid lines were drawn to guide the eye.

^{52}Mn spectrum from which a particular γ ray first appears. These beam energies were chosen in consideration of not only the physical thresholds involved but electronic thresholds as well, especially for the neutron detector. The target was a self-supporting ^{52}Cr foil of >99% isotopic enrichment and 0.68 mg/cm^2 in thickness. It was placed in a small chamber, specially designed to allow the 40-cm^3 coaxial Ge(Li) detector to be positioned about 2.5 cm from the target at 90°. The neutron detector was positioned at 90° from the beam direction, opposite the Ge(Li) detector, but a distance of about 10 cm from the target. The beam was tuned off the slits and after passing through the target, travelled down a 4-m section of beam tube before striking the Faraday cup. This ar-

TABLE II. Optical-model parameters. $r_c = 1.3$ all potentials.

Projectile	Nucleus	Energy (MeV)	V_0 (MeV)	r_0 (fm)	a_0 (fm)	W (MeV)	$4W_D$ (MeV)	r_i (fm)	a_i (fm)	χ^2	Reference
d	^{56}Fe	17	84.2	1.2	0.75	···	76.4	1.3	0.708	5.8	a
α	^{50}Ti	19.47	179.8	1.2	0.75	13.5	···	1.747	0.572	1.7	5, b

[a] Parameters obtained by J. D. Childs (to be published).
[b] R. Bock, P. David, H. H. Duhn, H. Hefele, U. Lynen, and R. Stock, Nucl. Phys. A92, 539 (1967).

rangement kept the γ-ray background from the tantalum slits and Faraday cup, low. Typical beam currents were 3 nA and run times ranged from 1 to 12 h at a given energy.

A description of the basic electronic circuitry, including pulse-shape descrimination on the NE 213 signal, has been given previously.[6] One difference, however, is the use of the Tennelec PACE four analog-to-digital converters (ADC's) interfaced to a PDP-15 computer in the present experiment. This allowed the event-by-event storage of four data parameters on magnetic tape, having 8192 channels assigned to each parameter. The parameters stored were Ge(Li) energy, neutron energy, time of flight (coincidence time), and pulse-shape signal. A gate over the neutron peak in the pulse-shape spectrum was necessary to reduce the accumulation of γ-γ coincidence data [Fig. 6(a), (b)]. The program CRUNCH[16] handled the logic necessary to run the ADC's and other peripherals. Because counting rates were kept low, the time spectrum showed ~200 : 1 true to accidental coincidence ratio. Although a time window of 100 nsec was set, most of the coincidence data fell within a time interval of ~25 nsec so no stripping over the time spectrum was necessary.

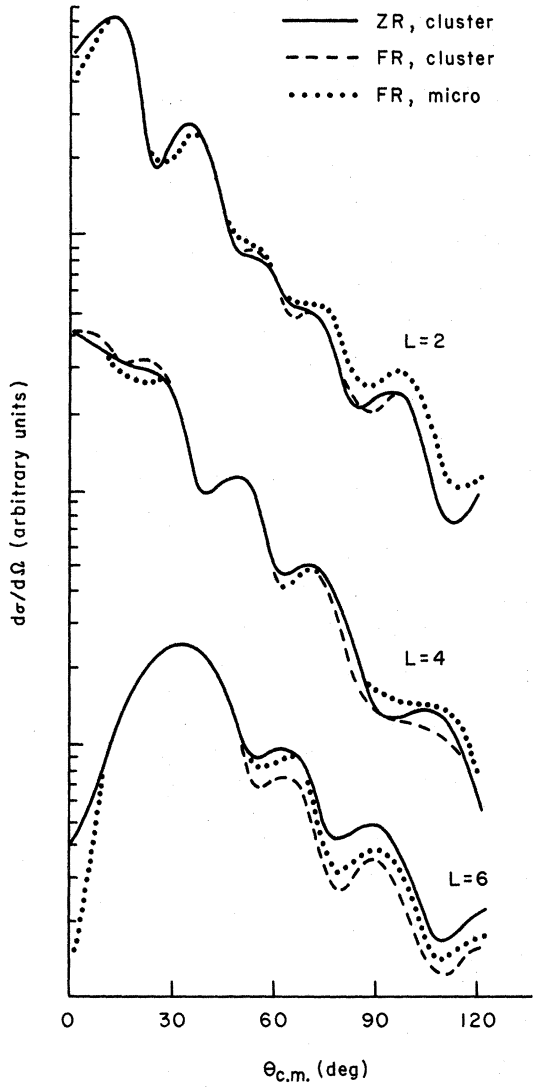

FIG. 3. DWBA curves for $^{54}Fe(d,\alpha)^{52}Mn$ at $E_d = 17$ MeV generated for an excitation of 1 MeV and arbitrarily normalized to each other. These show the effects of finite range and the cluster of microscopic deuteron description.

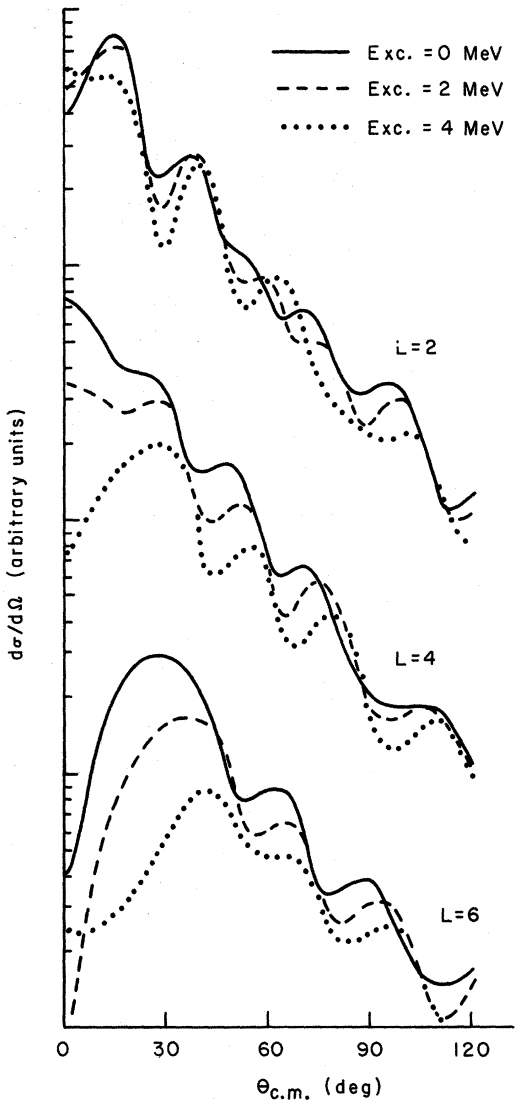

FIG. 4. DWBA curves for $^{54}Fe(d,\alpha)^{52}Mn$ at $E_d = 17$ MeV showing the Q-value dependence of the cross sections. The curves for a given L are absolutely normalized with respect to each other.

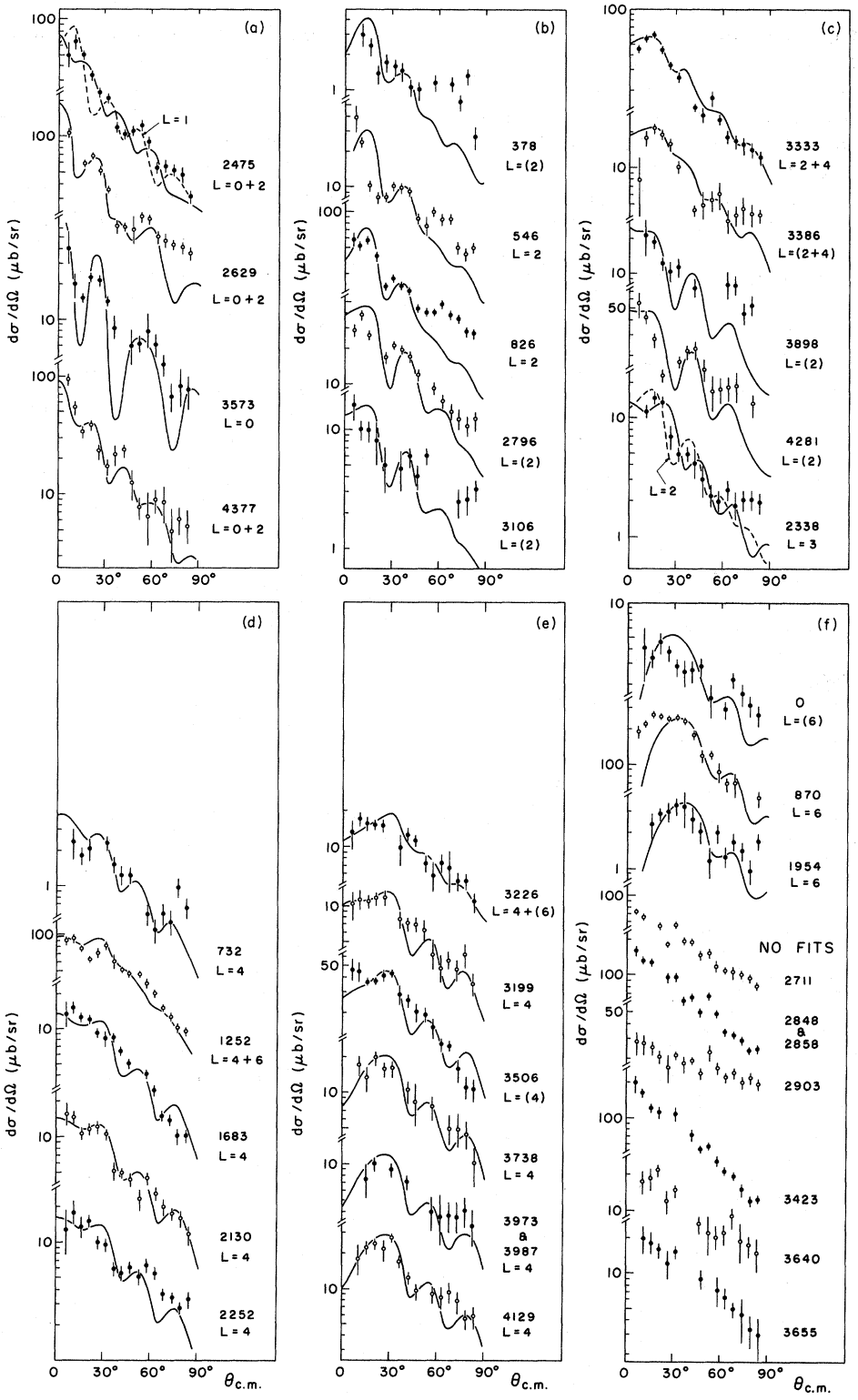

FIG. 5. (a)–(f) ^{54}Fe$(d,\alpha)^{52}$Mn angular distributions at $E_d = 17$ MeV. The curves are DWBA fits normalized to the data. Angular distributions are ordered according to increasing L transfer.

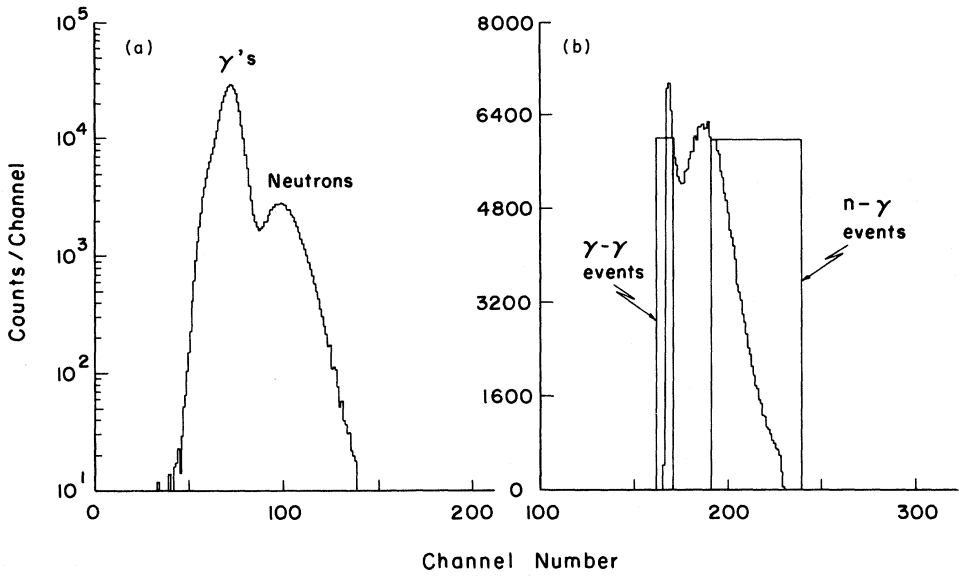

FIG. 6. Pulse-shape spectrum: (a) ungated and (b) gated and showing the regions over which the coincidence data were stripped.

B. Energy Determinations

The γ-ray energy resolution was 3 keV FWHM on the average. Energies were determined by means of standard calibration source spectra taken at different times during the run. The calibration points were least-squares-fitted to a polynomial of second order and the unknown energies determined from this. Figure 7 shows the γ-ray spectrum obtained at $E_p = 10$ MeV. The peaks are labeled with their energy. Singles γ-ray spectra were also taken at several energies. In these, the ^{52}Cr γ rays[17] provided an internal calibration. The energies given in Fig. 7 and Table III are based on averages of all the coincidence and singles data and are believed accurate to ±0.5 keV except where indicated.

C. Identification of ^{52}Mn γ Rays

Relative photopeak intensities are given in Table III. These are considered accurate to ±25% for

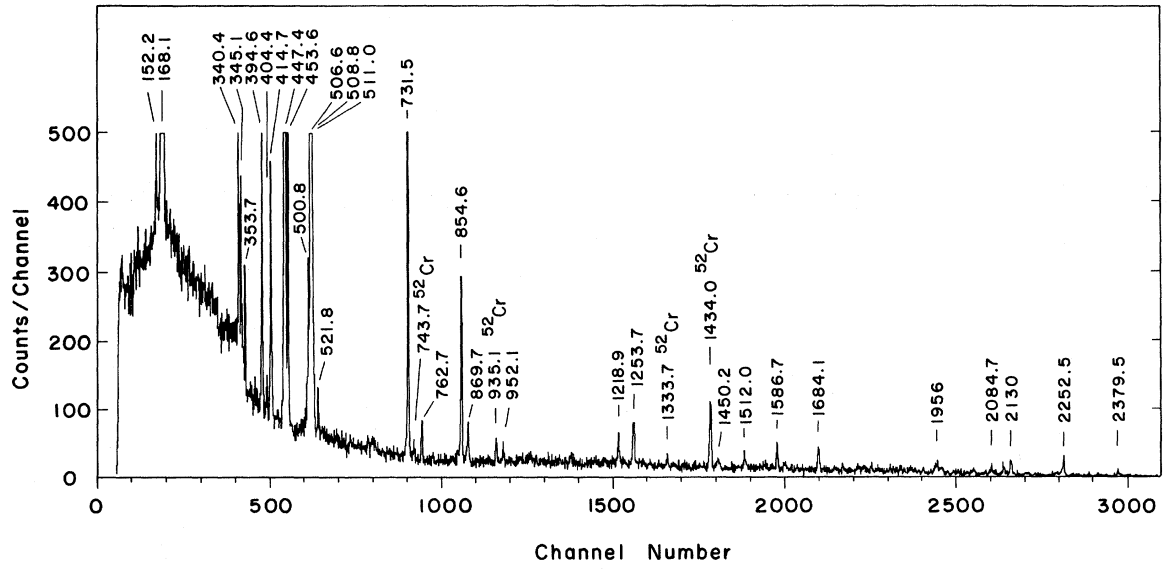

FIG. 7. ^{52}Cr$(p,n\gamma)^{52}$Mn coincidence γ-ray spectrum at $E_p = 10$ MeV.

TABLE III. Coincidence γ rays. Energies and relative photopeak intensities, I, corrected for Ge(Li) efficiency.

E_γ (keV)	Singles I average of E_p = 9 and E_p = 10 MeV runs	Coincidence I E_p = 10 MeV	Coincidence I E_p = 9.5 MeV	Coincidence I E_p = 9 MeV	Coincidence I E_p = 8.5 MeV	Coincidence I E_p = 8 MeV	Singles/ Coincidence E_p = 10 MeV	Contaminants
152.2	3.7	3.1	2.5	2.0	1.4	5.5	0.7	
168.1	97.6	70.6	53.0	83.0	106.0	446.0	1.4	
340.4	7.2	9.4	10.0	11.3	8.4	13.4	0.8	
345.1	6.7	7.6	8.1	7.3	3.5		0.9	
353.7	5.9	5.6	4.8	5.0	4.2	8.1	1.1	
394.6	15.4	19.3	12.3	10.2	2.5		0.8	
404.4	1.2	2.0	1.7	0.6			0.6	
414.7	12.3	18.0	8.9	5.4			0.7	
447.4	100.0 [a]	100.0 [a]	100.0 [a]	100.0 [a]	100.0 [a]	100.0 [a]	1.0	
453.6	24.4	29.3	16.7	14.0	4.2		0.8	
500.8	(24)	18.4	17.0	15.3	6.3		1.3	
506.6	(165)	(108)	(90)	(103)	(77)	(105)	1.5	
508.8	(630)	(86)	(71)	(91)	(77)	(143)	7.3	Some 511.0
521.8	2.9	4.2	2.4	1.9			0.7	
731.5	59.6	64.9	47.7	57.0	45.3	88.9	0.9	
743.7	35.7	3.4	1.7	1.0	1.0	10.4	10.5	^{52}Cr
762.7	1.5	6.4	4.8	2.7			0.2	
854.6	33.1	39.5	37.6	30.8	15.8		0.8	
869.7	b	9.7	2.7	2.0	0.6			
935.1	98.5	4.3	4.4	3.4	3.5	11.9	23	^{52}Cr
952.1		4.2	2.6					
1218.9		6.2	6.3					
1253.7	10.7	17.7	9.6	10.4	1.7		0.6	
1333.7	84.8	2.1	2.2	2.5	1.2	8.6	40	^{52}Cr
1434.0	910.0	28.1	17.4	15.2	21.8	62.4	32	^{52}Cr
1450.2		6.0	0.9					
1512.0	7.2	7.4	1.5				1.0	
1586.7	12.8	12.8	1.9				1.0	
1684.1	9.0	13.6	3.8	1.8			0.7	
1956 ± 2 [c]		8.7	2.5					
2084.7		6.1						
2130 ± 2 [c]		14.1	2.5					
2252.5	23.6	14.5	2.8				1.6	
2379.5	21.7	3.1					7.0	

[a] Intensities normalized to this γ ray.
[b] Blanks denote not seen. Could be present but weak.
[c] Possible doublet.

the stronger peaks and ±50% to +100% for the weaker ones. These errors are due largely to background-subtraction uncertainties. A large value of the singles/coincidence intensity ratio shown in Table III is indicative of ^{52}Cr γ rays getting through the gates and indeed several such γ rays have been identified in the table. The high ratio for the γ ray at 2379.5 keV, is, however, due to a threshold effect. It can be seen from the table that when a γ ray first appears its intensity is usually significantly lower than the intensity it reaches as the beam energy is raised. Another method of identifying ^{52}Mn γ rays is to strip the data over the regions of the pulse-shape spectrum shown in Fig. 6(b), i.e., selecting γ-γ event data and n-γ event data. This method confirms the identifications made in Table III. The 506.6- and 508.8-keV γ rays are so close to the 511.0-keV annihilation γ ray that their genuineness may be questioned. Figure 8 shows a detailed plot of this portion of the spectrum for the two strips of Fig. 6(b). In the γ-γ event data where the 511-keV γ ray should be strongest, the 508.8-keV γ ray is replaced by another γ ray of slightly, but noticeably, higher energy. This higher energy is 510.4 keV which makes it a reasonable candidate for the 511. Hence the apparently high singles/coincidence ratio for the 508.8-keV γ ray can be explained.

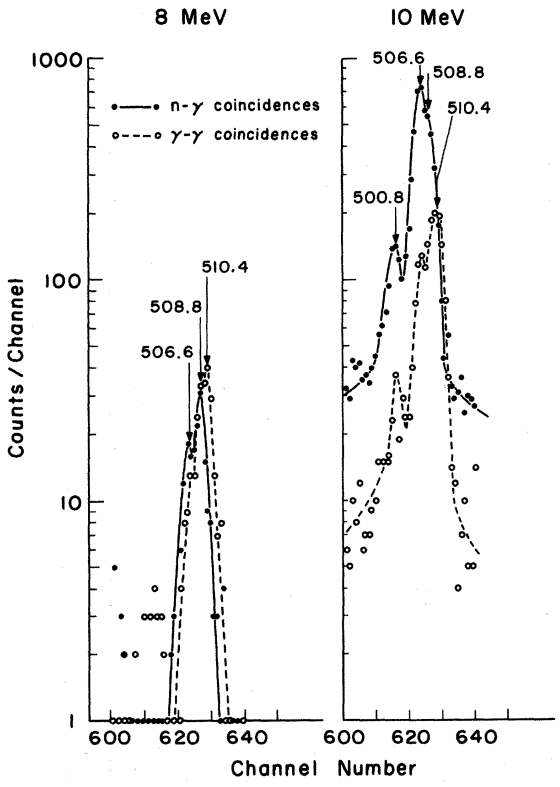

FIG. 8. Details of the γ-ray triplet at 508 keV.

D. Construction of the Decay Scheme

Using the data of Table III, it is not possible to construct a decay scheme with only the known levels of ^{52}Mn (Table I). Difficulties occur even at low excitation. However, because of the abundance of γ rays, new levels can be produced which satisfy energy and intensity balances. Considering the threshold for the first appearance of a γ ray and allowing for the possibility that high-spin states are not significantly excited until well above threshold (for example the 7^+ state), the decay scheme of Fig. 9 is proposed. Except for the 7^+ state, the beam energies shown in the figure are positioned such that all γ rays drawn below this position are seen at this beam energy. The 377.8-keV γ ray did not appear in the gated spectra (21.3-min half-life). The energy of this level was taken from Ref. 18, however, a γ ray of 377.7 keV appeared in the singles spectrum. The decay scheme of Fig. 9 satisfies energy balances, usually well within the errors.

The proposed new levels are at 886.5, 1232.4, and 1278.9 keV. The close proximity of the 886.5-keV level to the 884.4-keV level precludes its identification in the particle spectra. The 1232.4- and 1278.9-keV levels are about 20 keV away on either side of the 1253.5-keV level. Their appearance was not evident in the (^{3}He, t) spectra. The 1253.5-keV level was reported as a doublet in the (d, α) work of Ref. 11. It was therefore decided to rescan this portion of the (d, α) plate spectra in finer steps. The results are shown in Fig. 10. Two rather weak levels are present which do not kinematically shift with angle relative to the 1253.5-keV level. The impurity peaks shift by about 2 mm over this same angular range. Their energies are found to be 1232 ± 2 and 1280 ± 2 keV in good agreement with the γ-ray data.

Based on this decay scheme, the energies of many of the ^{52}Mn levels can be determined quite accurately as given in Fig. 9 and Table IV where the errors are also estimated. Table IV also shows the spin limits of these levels assuming that the γ-ray transitions proceed by a multipolarity of 2 or less. These are perfectly compatible with the particle-transfer results.

DISCUSSION AND CONCLUSIONS

For most of the ^{52}Mn levels studied in (d, α), L transfers could be assigned or suggested. Considering that DWBA often encounters difficulties when applied to low-mass nuclei, the fits shown

in Fig. 5 are reasonable. The (d, α) normalization constant based on the assumption that the 870-keV 7^+ state is a pure $f_{7/2}$-shell state is found to be $N(d, \alpha) = 2220$. The procedure employed in Ref. 5 which included finite-range corrections was used to obtain this value. It is in line with the ^{52}Cr-(d, α) and ^{58}Ni(d, α) normalizations reported there. $N(d, \alpha)$ is sensitive to the DWBA procedure used.

The angular distributions shown here are not as structureless as those previously reported by Kelleter *et al.*[4] taken at $E_d = 15$ MeV. This may result from the fact that the data of Ref. 4 did not include low angles where much of the (d, α) structure appears. For example the 546-keV level would lack much of its structure if the data $\leq 15°$ c.m. were absent in Fig. 5. The possibility that compound effects are present for this level at $E_d = 15$ MeV would not be supported by the excitation function shown in Fig. 2. Kelleter *et al.* see the 2475-keV level (reported as 2498 keV by Ref. 4) as proceeding by $L = 1 + 3$. The angular distribution for this level shown in Fig. 5 could be easily fitted by $L = 1$ (dotted line). However, the definite $L = 0$ transfer seen in $(^3$He, $p)$ for a level at 2471 keV [12] indicates either that this a 1^+ level proceeding by $L = 0 + 2$ (solid line in Fig. 5) or that

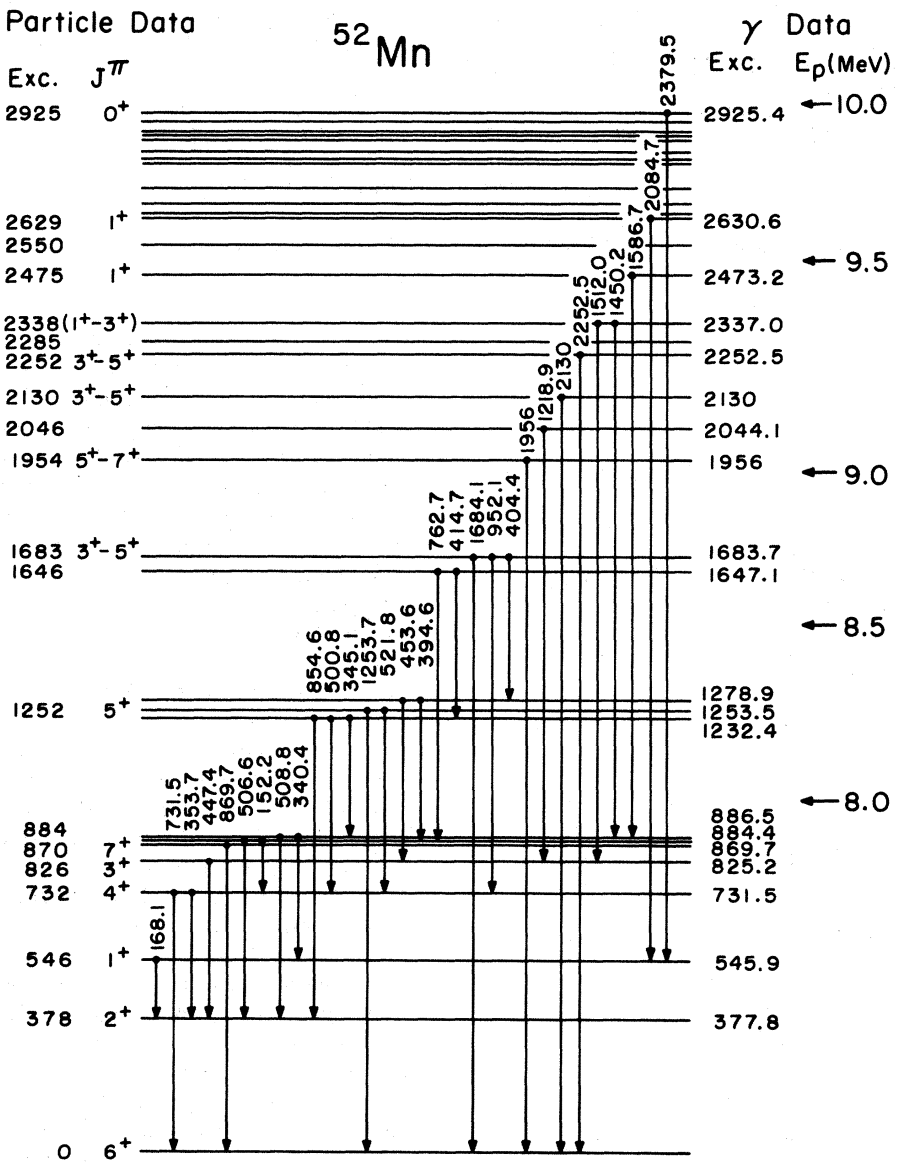

FIG. 9. ^{52}Mn decay scheme from the ^{52}Cr$(p, n\gamma)^{52}$Mn reaction.

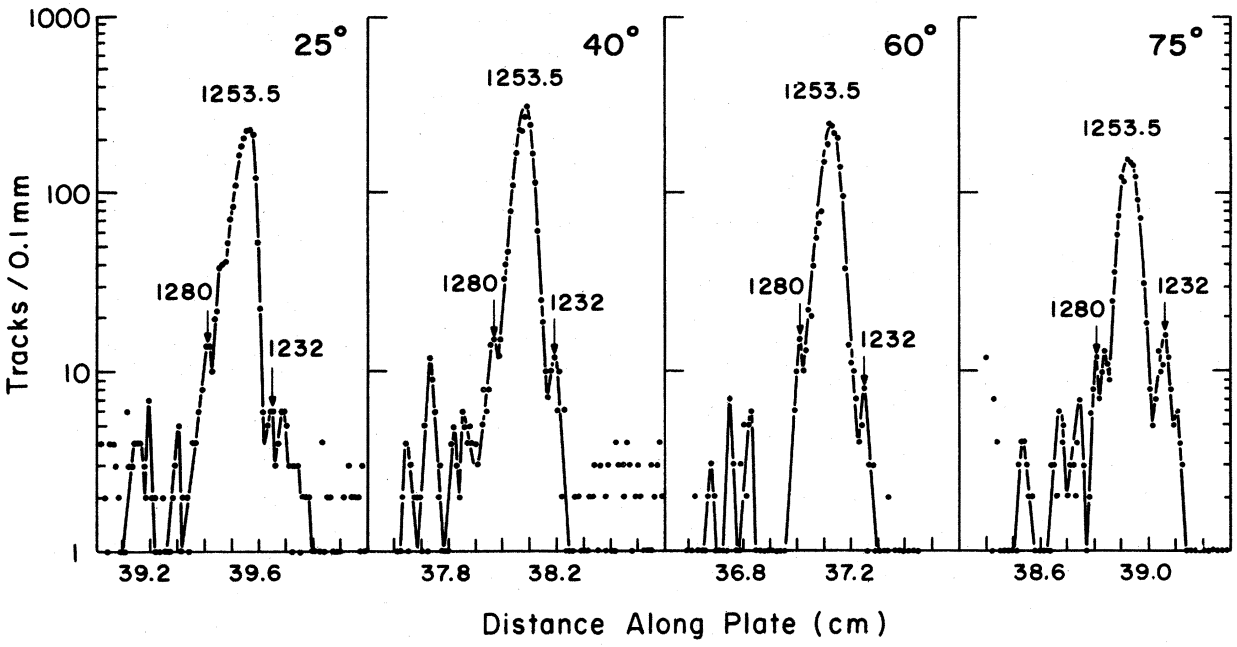

FIG. 10. Rescan of the 1253-keV region of the ^{54}Fe$(d,\alpha)^{52}$Mn plates in 0.1-mm steps.

TABLE IV. Data on ^{52}Mn levels which participate in the decay scheme of Fig. 9.

Exc. (keV)	J^π particle data	J γ data [a]
0.0	6^+	b
377.8 ± 0.2	2^+	b
545.9 ± 0.2	1^+	b
731.5 ± 0.2	4^+	4
825.2 ± 0.5	3^+	b
869.7 ± 0.5	7^+	b
884.4 ± 0.5		2–4
886.5 ± 0.5		0–3
1232.4 ± 0.5		2–4
1253.5 ± 0.5	5^+	4–6
1278.9 ± 0.5		2–5
1647.1 ± 0.5		
1683.7 ± 0.5	$3,4,5^+$	4–6
1956 ± 2	$5,6,7^+$	≥4
2044.1 ± 1		1–5
2130 ± 2	$3,4,5^+$	≥4
2252.5 ± 0.5	$3,4,5^+$	≥4
2337.0 ± 0.5	$(1^+\text{-}3^+)$	1–5
2473.2 ± 2	1^+	0–5
2630.6 ± 1	1^+	0–3
2925.4 ± 1	0^+	0–3

[a] Assuming a multipolarity of 2 or less.
[b] J^π assumed from particle data.

there is a close doublet at 2475 keV, one member of which is excited in (d, α) and the other (possibly a 0^+ level) in $(^3\text{He}, p)$. Since the $(p, n\gamma)$ reaction, which is expected to excite low-spin states, shows no evidence for a doublet at this energy the 1^+ assignment for this level is preferred.

Our excitation energies agree with Kelleter's for levels below 1 MeV. For higher excitations it appears that Kelleter's energy assignments are systematically ~25 keV too high. This was taken into account in the comparisons shown in Table I where it will be seen that the (d, α) L transfers of this work agree with Kelleter's wherever a comparison is possible, except for the 2475-keV level noted above.

The ±30-keV energy uncertainty in the (d, α) work of Guichard *et al.*[3] at $E_d = 28$ MeV makes a comparison difficult for the levels at high excitation in ^{52}Mn. Assuming the correspondence shown in Table I to be correct, there are very few disagreements. Guichard's $L = (2)$ suggestion for the level at 2130 keV (2.15 MeV in Guichard's work), contrasts with the definite $L = 4$ angular distributions shape in Fig. 5. According to the γ-ray work reported here, this level should have $J \geq 4$ (Table IV), since it decays to the 6^+ ground state. This rules out the $L = 2$ possibility in (d, α). The 80-keV resolution of Guichard's data makes the few remaining disagreements difficult to resolve except to suggest that in view of the increasing density of states the probability that more than one

level contributes to an angular distribution becomes significant.

Our data are in accord with the (^{3}He, p) data[11, 12] except for the 3199-keV level. The $L=0$ (^{3}He, p) transition to a level at 3213 keV may not correspond to the (d, α) level. If the 3213-keV level were 0^+ it would not be seen in (d, α). In view of the energy uncertainty of $\leq \pm 10$ keV in Ref. 12, this is likely to be a separate level.

The present (d, α) results agree with the (^{3}He, t) data[13] except for the 2629-keV level. However, as pointed out in Ref. 12 this may be the result of energy uncertainties in the (^{3}He, t) data. The assignments of Ref. 18 shown in Table I are also compatible with our data.

The level at 2925 keV has previously been identified as the isobaric analog of the ^{52}Cr ground state.[19, 20] The large (^{3}He, t) cross section measured here at 40° lab together with the absence of this level in (d, α) supports this identification.

The excellent agreement of the ^{52}Mn energy assignments based on the particle data (Table I) with the energies determined by the γ-ray data (Table IV) is noteworthy. The direct-comparison technique employed here should be a reliable one provided the level energies in the calibration spectrum are accurately known.

The column labeled "best J^π" in Table I incorporates the results of all the particle data. The γ-ray data is in accord with these J^π assignments (assuming multipolatities ≤ 2). The spins of most of the low-lying states are known so that a comparison with the recent MBZ calculation[21] is possible as shown in Fig. 11. The four new levels reported here (for which no definite spin-parity assignments are known) do not appear to fit into the MBZ scheme. The next higher MBZ level is predicted above 2 MeV. The agreement of the other experimental levels with theory is quite good in view of expected theoretical energy uncertainties of ~250 keV.[1] The agreement shown here appears to be an improvement over their earlier predictions for this nucleus (see Ref. 4.)

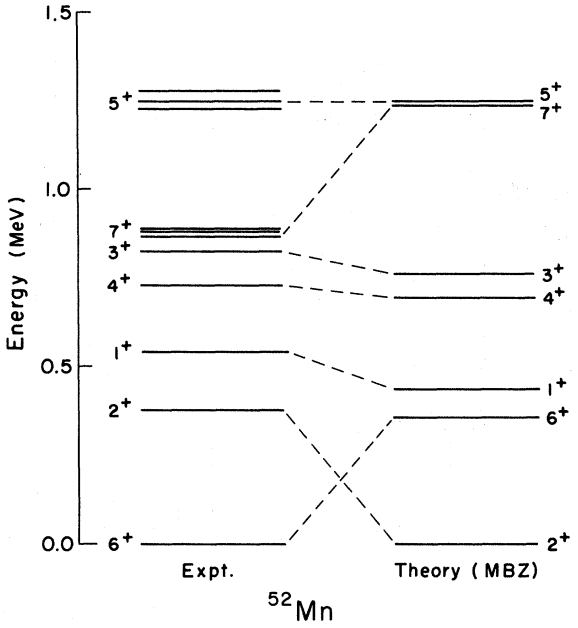

FIG. 11. Comparison of the experimental data with the MBZ calculations for ^{52}Mn.

In particular the order of the 3^+ and 4^+ levels is now correct. If the new levels have negative parity, they would not be expected to fit into the $f_{7/2}$-shell scheme. If they have positive parity, it would indicate that configuration mixing may be important in ^{52}Mn at relatively low excitation. They could also possibly be collective levels.

ACKNOWLEDGMENTS

It is a pleasure to acknowledge R. F. Gibson and M. J. Spisak for much help in the data acquisition and to thank J. D. Childs for the use of his code SPIRO and the ^{56}Fe optical-model parameters before publication. The author wishes to thank Professor W. W. Daehnick for many valuable discussions concerning all aspects of this work and for a reading of the manuscript.

---

*Work supported by the National Science Foundation.

†Present address: Physics Department, Princeton University, Princeton, New Jersey 08540.

[1]J. D. McCullen, B. F. Bayman, and L. Zamick, Phys. Rev. 134, B515 (1964).

[2]N. K. Glendenning, Ann. Rev. Nucl. Sci. 13, 191 (1963).

[3]A. Guichard, M. Chevallier, P. Gaillard, J.-Y. Grossiord, M. Gusakow, J.-R. Pizzi, and C. Ruhla, Nucl. Phys. A164, 56 (1971).

[4]H. Kelleter, D. Bachner, B. Schmidt, and W. Seliger, Nucl. Phys. A183, 509 (1972).

[5]R. M. DelVecchio and W. W. Daehnick, Phys. Rev. C 6, 2095 (1972).

[6]R. DelVecchio, R. F. Gibson, and W. W. Daehnick, Phys. Rev. C 5, 446 (1972).

[7]M. J. Schneider and W. W. Daehnick, Phys. Rev. C 4, 1649 (1971).

[8]M. J. McEllistrem, K. W. Jones, and D. M. Sheppard, Phys. Rev. C 1, 1409 (1970).

[9]S. Maripuu, Nucl. Phys. A149, 593 (1970).

[10]Written by J. D. Childs (unpublished).

[11]J. Rapaport, W. E. Dorenbusch, and T. A. Belote, Nucl. Phys. A109, 657 (1968).

[12]O. Hansen, T. J. Mulligan, and D. J. Pullen, Nucl.

Phys. A167, 1 (1971).
[13]G. Bruge, A. Bussiere, H. Faraggi, P. Kossanyi-Demay, J. M. Loiseaux, P. Roussel, and L. Valentin, Nucl. Phys. A129, 417 (1969).
[14]Written by P. D. Kunz, 1969 (unpublished), 2nd version.
[15]W. W. Daehnick and Y. S. Park, Phys. Rev. 180, 1062 (1969).
[16]Written by J. J. Kolata, R. F. Gibson, and J. Holden (unpublished).
[17]C. F. Monahan, N. Lawley, C. W. Lewis, I. G. Main, M. F. Thomas, and P. J. Twin, Nucl. Phys. A120, 460 (1968).
[18]J. Rapaport, Nucl. Data B3 (Nos. 5 and 6) (1970).
[19]R. Sherr, A. G. Blair, and D. D. Armstrong, Phys. Letters 20, 392 (1966).
[20]M. Harchol, A. A. Jaffe, J. Miron, I. Unna, and J. Zioni, Nucl. Phys. A90, 459 (1967).
[21]H. Ohnuma and A. M. Sourkes, Phys. Rev. C 3, 158 (1971), and references therein.

PHYSICAL REVIEW C VOLUME 7, NUMBER 2 FEBRUARY 1973

Straight-Back Elastic Alpha Scattering from ^{48}Ti, ^{52}Cr, ^{53}Cr, and ^{58}Ni†

P. T. Sewell and J. C. Hafele*
Department of Physics, Washington University, St. Louis, Missouri 63130

and

C. C. Foster and N. M. O'Fallon
Department of Physics, University of Missouri-St. Louis, St. Louis, Missouri 63121

and

C. B. Fulmer
Oak Ridge National Laboratory,‡ Oak Ridge, Tennessee 37830
(Received 11 February 1972)

Cross sections are reported for α particles scattered from ^{58}Ni, ^{52}Cr, ^{53}Cr, and ^{48}Ti. For the ^{58}Ni target, both elastic and inelastic (to the first excited state) data are presented for α particles of 12 incident energies between 13 and 29 MeV scattered into the angular range from 152° through 180° to −172°. Elastic excitation functions at 180° are given for α particles of six energies between 20 and 29 MeV scattered from ^{52}Cr, ^{53}Cr, and ^{48}Ti. The elastic angular distributions exhibit a narrow "glory peak" at 180° for each energy, and the peak cross section at 180° is sensitively dependent on both the bombarding energy and the target mass. For the case of ^{58}Ni, the measured elastic cross sections at 180° are about an order of magnitude larger than values predicted from optical-model calculations with a potential that fits α scattering data forward of 140°.

I. INTRODUCTION

Although the nuclear optical model has been used successfully for years to fit elastic scattering data for a variety of projectiles and targets, the resulting optical potentials for complex projectiles are usually highly ambiguous.[1,2] It is generally possible to find several optical potentials, differing mostly in the real well depth, which produce acceptable fits to data. The continuous Vr^n ambiguity is also a well-known problem.

Singh *et al.*[3] found that optical-model analysis of their ^{24}Mg(α, α) data between 20 and 170° at 40 MeV yielded four families of parameters which gave acceptable fits, while analysis of 80-MeV data resulted in only one acceptable family. When only forward-angle data (<70°) at 80 MeV were fitted, again four parameter families were found. Fulmer and Hafele[4] analyzed ^{27}Al(h,h) data back to ≈165° at 59.8 and 29.6 MeV. Both discrete family and continuous ambiguities were present when the lower-energy data were analyzed. When the higher-energy data were fitted, discrete ambiguities were eliminated and continuous ambiguities were markedly reduced. Analysis of only the higher-energy data forward of 70° brought back the discrete ambiguities.

A number of measurements of elastic α scattering have shown a strong increase in cross section with well-defined oscillations at large angles. References 5 through 9 report such measurements for target A in the range 39 through 70, α energies of 18 to 40 MeV, and scattering angles back as far as 160 to 179° in the center of mass.